

## Particle Interaction Measurements in a Coulomb Crystal Using Caged-Particle Motion

R. A. Quinn\* and J. Goree†

*Department of Physics and Astronomy, The University of Iowa, Iowa City, Iowa 52242*

(Received 29 May 2001; published 24 April 2002)

A technique for characterizing the particle interaction potential of a Coulomb crystal is developed. The mean-square displacement (MSD) is measured, showing both caged- and superdiffusive-particle motions. By subtracting the center of mass of neighboring particles in computing MSD, only short-wavelength particle motions are retained. This yields the lattice Einstein frequency, which contains information about the interparticle forces and potentials. Video measurements of particle motions in a complex (dusty) plasma are used to demonstrate the technique.

DOI: 10.1103/PhysRevLett.88.195001

PACS numbers: 52.27.Lw, 82.70.Dd

Coulomb crystals have been studied for many years and can be thought of as models for natural crystals. A Coulomb crystal is a system of mutually repulsive particles that has self-organized into a lattice structure under the influence of an external confinement. It exhibits many of the same properties as ordinary crystals, such as the development of topological defects and phase transitions during heating. Thus, a detailed study of the properties of a Coulomb crystal yields useful information about ordinary crystals.

Here, we describe a technique for characterizing the particle interaction potential in a Coulomb crystal. The methodology is generally applicable since it requires only measurement of the mean-square displacement (MSD) of the particles in the lattice, as a function of time. Particles in a crystal, or a highly ordered or freezing liquid, cannot diffuse freely but are trapped at short times by the “cage” formed by the neighboring particles.

We filter out the particle motion associated with long-wavelength phonons by computing the MSD of a particle relative to the center of mass of the neighboring particles. What remains are short-wavelength phonons which yield information about the interparticle forces and potentials through the Einstein frequency  $\omega_E$ .

We demonstrate this technique using a two-dimensional (2D) experimental model system called a complex (or dusty) plasma. The complex plasma, so called in analogy with complex fluids, consists of a suspension of highly charged particles in a background plasma of ions and electrons and confined by external electric fields. The particle motions are damped by collisions with the neutral background gas, and phase transitions are frequently driven by changing the neutral gas pressure [1,2]. Complex plasmas are similar to aqueous colloidal suspensions [3] but have damping rates and volume fractions which are smaller by a factor of up to  $10^5$ . The ambient plasma plays several roles: it sustains a negative charge on the particles, it provides a sort of Debye shielding in the vicinity of the particles, and

it provides an inward long-range electric force  $F_{\text{ext}}$  that confines the mutually repulsive particles in a stable suspension. The suspension is characterized by direct measurements of the particle locations which yield structural, such as topological defect statistics, as well as dynamical information.

In the time domain, the dynamical measurements we report here are  $\text{MSD}(t)$  and the mean-square velocity  $\langle v^2 \rangle$ . In previous experiments,  $\text{MSD}(t)$  has revealed diffusive and superdiffusive motion at long times [4]; our data show this as well, but we add analysis of short-time caged (oscillatory) motions, from which we also derive  $\omega_E$ . Note that it is possible to measure the MSD not only from direct measurements of particle positions, as we have done, but also, e.g., using dynamic light scattering in complex fluids [5]. In the frequency domain, dynamical measurements can also be made [6]; however, the spectra do not yield  $\omega_E$  in a straightforward way.

Information about the interparticle potential is embedded in the MSD through the particles’ caged motions. The equation of motion for a caged particle can be modeled with a single-particle Langevin equation:

$$\frac{d^2x}{dt^2} = -\omega_E^2 x - \nu \frac{dx}{dt} + \frac{1}{m} \xi(t). \quad (1)$$

Here,  $x(t)$  is the coordinate of a single particle,  $m$  is the particle mass,  $m\nu dx/dt$  is the drag force due to the neutral gas,  $m\omega_E^2 x$  is the springlike force due to the cage of the neighboring particles, and  $\xi(t)$  is a random, fluctuating force that heats the particle [7]. The lattice Einstein frequency  $\omega_E$  is obtained from a Taylor series expansion of the net force on a particle due to the particles around it. In turn, the net force depends on the interparticle potential and lattice configuration.

Equation (1) is the equation of motion for a driven, damped harmonic oscillator, and it can be solved for  $\text{MSD}(t) \equiv \langle x^2/a^2 \rangle$  yielding

$$\text{MSD}(t) = \frac{\langle v^2 \rangle}{a^2 \omega_E^2} \left\{ 1 - \exp(-\nu t/2) \left[ \cosh(\nu_0 t) + \frac{\nu}{2\nu_0} \sinh(\nu_0 t) \right] \right\}, \quad (2)$$

where  $\nu_0 = (\nu^2/4 - 2\omega_E^2)^{1/2}$  and  $a$  is the mean interparticle spacing. Equation (2) is the solution for overdamped oscillations, corresponding to  $\nu_0^2 > 0$ . In the underdamped case of sinusoidal motion,  $\nu_0^2 < 0$ , Eq. (2) should be modified by replacing  $\nu_0$  with  $i\nu_0$ . Since we can measure  $\text{MSD}(t)$ ,  $\langle v^2 \rangle$ , and  $\nu$ , we can extract  $\omega_E$  from Eq. (2).

The following assumptions have been made in Eq. (1) and its solution Eq. (2): (i) The particle is permanently trapped in its cage. (ii) Its neighboring particles do not move ( $\omega_E = \text{const}$ ). (iii) The random force  $\xi(t)$  is uncorrelated with the particle position for all times,  $\langle x\xi \rangle = \langle x \rangle \langle \xi \rangle = 0$ . (iv) The thermal velocity  $\langle v^2 \rangle$  is independent of time and is related to the random force  $\langle v^2 \rangle \propto \langle \xi^2 \rangle$  (see Ref. [7] for a detailed discussion of this point).

An experimental determination of  $\omega_E$  yields information about the interparticle force and potential, as we now discuss. The binary interaction force is  $\mathbf{F}_i = -\nabla\phi_i$ , where  $\phi_i$  is the interparticle potential. This pairwise force should be summed over all of the neighboring particles. Including a contribution due to the overall confining electric field  $\mathbf{F}_{\text{ext}}$  yields the total net force on the caged particle. The external confinement is radially inward and acts to hold the repulsive particles together. When a particle is at its equilibrium position, at the center of its near-neighbor cage,  $\mathbf{F}_{\text{net}} = \sum_{i=1}^{N-1} \mathbf{F}_i + \mathbf{F}_{\text{ext}} = 0$ , where  $N$  is the number of particles in the lattice. For small displacements  $\delta r$  in any direction  $\hat{r}$ ,  $\mathbf{F}_{\text{net}} = -(\omega_E^2 + \omega_{\text{ext}}^2)\delta r\hat{r}$ . Here,  $\omega_{\text{ext}}$  represents a global or rigid-body oscillation mode of the whole crystal in the external confinement. In most experiments, including the present one,  $\mathbf{F}_{\text{ext}}$  is very flat near the particle locations, so that  $\omega_{\text{ext}}^2 \ll \omega_E^2$ , and can be neglected. Thus, we have

$$\omega_E^2 = 1/m \sum_{i=1}^{N-1} \partial \mathbf{F}_i / \partial x, \quad (3)$$

where the displacement  $\delta r$  is now taken to be along the (arbitrarily oriented)  $x$  axis.

We conducted an experiment using a quasi-two-dimensional complex plasma in which we have determined  $\omega_E$  by examining the MSD of the particles. The complex plasma consisted of two to three layers of microspheres levitated and confined in the sheath of an rf plasma. The particles were highly negatively charged due to the collection of the plasma electrons and ions which also acted to partly shield the interaction potential. The plasma itself was sustained in a low-density neutral argon gas. Further details on the experimental setup are given in Ref. [8].

In addition to supplying the source for plasma ions and electrons, the neutral gas also damps the particle motions through frictional drag. In our parameter regime, i.e., neutral gas pressures between 220 and 500 mTorr, the neutral gas damping rate  $\nu$  is due to Epstein drag [9,10]. The effect of this drag is to cool the particles, at the same time that electrostatic instabilities act to heat them [7,11,12]. The particles form a solid phase at the highest pressures

and a liquid phase at the lower pressures. Caging is imperfect in the liquid phase where particles tend to diffuse more easily.

For monolayer complex plasmas, the interparticle potential is Yukawa [13]. Here, we have a multilayer system. Particles in the various layers are vertically aligned due to an anisotropy in the interaction potential which arises from the ion focus phenomenon [14,15]. In effect, our particles are like short vertical rods that move only in the horizontal direction. The exact form of the inter-rod potential has not been measured, but calculations of the *interparticle* potential indicate a shielded Coulomb interaction [16], which suggests that the inter-rod potential is roughly Yukawa. The two dimensionality of the system was verified by the observation of strongly aligned vertical columns of particles which moved together in the horizontal direction [17].

Structural and dynamical measurements of the particles were made by shining a laser sheet through the upper layer of the particle suspension and imaging the particles with a video camera. We identified and tracked  $\sim 800$  particles for up to 20 s at each of 11 neutral gas pressures during the transition. For comparison, the total particle suspension contained  $\sim 40000$  particles. A Voronoi analysis was performed to identify nearest-neighbor bonds and topological defects in the lattice. By tracking the particles from frame to frame, velocity measurements were made, yielding the particle kinetic temperature [8].

We computed  $\text{MSD}(t)$  from the particle trajectories as follows:

$$\text{MSD}(t) = \frac{1}{Na^2} \sum_{i=1}^N [\mathbf{x}_i(t) - \mathbf{x}_{\text{CM}}(t)]^2. \quad (4)$$

Here,  $\mathbf{x}_i(t)$  is the trajectory of the  $i$ th particle position vector,  $\mathbf{x}_{\text{CM}}(t) = 1/n_n \sum_{j=1}^{n_n} \mathbf{x}_j(t)$  is the center of mass (CM) of the  $i$ th particle's nearest neighbors,  $n_n$  is the number of nearest neighbors (usually  $n_n = 6$ , except for defects), and  $N$  is the total number of particles tracked. The  $n_n$  nearest neighbors are identified at time  $t = 0$ , and the same ones are used to compute the CM at all future times, even if they cease to be nearest neighbors of particle  $i$ . Thus, at longer times  $\text{MSD}(t)$  measures the tendency of a particle to escape its near-neighbor cage. At shorter times it measures caged-particle motion.

Our method of subtracting the center of mass of the neighboring particles in Eq. (4) achieves two purposes. First, it filters out the long-wavelength components of the phonon spectrum. Second, it eliminates the affect of secular motion of the particles.

The MSD curves in Fig. 1 show both caged- and diffusive-particle motion. The curves are plotted as a time series, where time is normalized by  $\nu^{-1}$ . Caged motion occurs roughly for  $t\nu < 100$ , while superdiffusive motion occurs at longer times. We deduce this by comparing the slopes of the curves in Fig. 1(a) in the two time regimes. At long times, the log-log slopes are  $> 1$  and characteristic

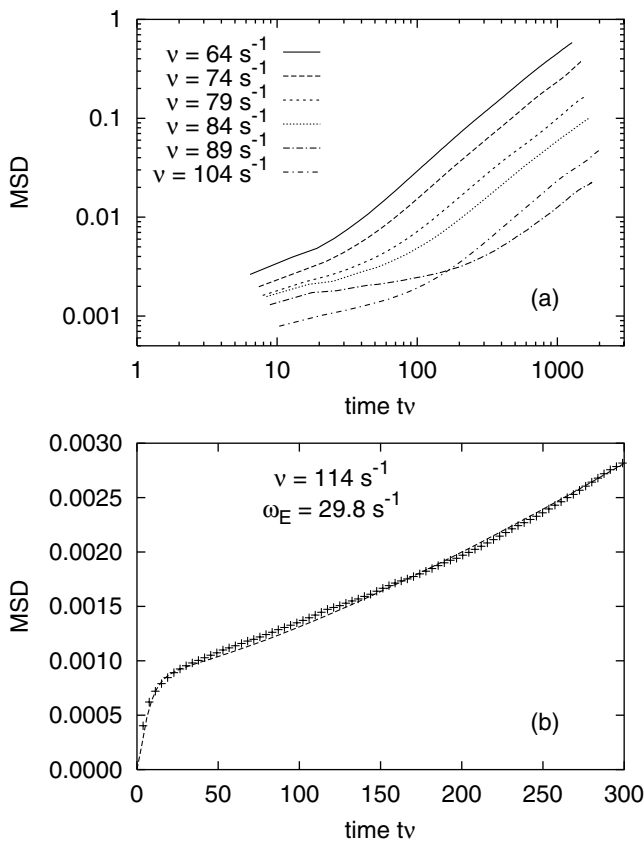


FIG. 1. Mean-square displacement (MSD) versus time normalized by the inverse damping rate ( $\nu^{-1}$ ) on a log-log scale. (a) Curves are shown for six representative neutral gas pressures (damping rates  $\nu$ ) during the melting transition. The small slopes of the curves for  $tv < 100$  indicate that the particle motion is caged. (b) A representative MSD curve is shown with a fit to Eq. (2) plus a diffusionlike term. The fit yields the lattice Einstein frequency ( $\omega_E$ ), after using the separately measured particle kinetic energy  $m\langle v^2 \rangle$ ,  $\nu$ , and interparticle spacing  $a$ . Note that here the axes are not log scale and the time resolution is higher than in (a).

of superdiffusive-particle motion while at short times the slopes are  $\ll 1$ . We identify the short-time behavior as caged-particle motion.

We found the lattice Einstein frequency  $\omega_E$  from the MSD in the caged regime. The technique is illustrated in Fig. 1(b), which shows an expanded view of the caged regime for  $\nu = 113.5 s^{-1}$ . Here, we have fit the measured MSD to Eq. (2) plus a quasidiffusive term,  $Dt^b$ . The parameters  $\langle v^2 \rangle$ ,  $m$ , and  $\nu$  were measured or computed from other data. The  $6.5 \mu m$  diameter particles had a mass  $m = 2.2 \times 10^{-10}$  g, and the particle temperature  $T_p = m\langle v^2 \rangle$  ranged from 0.06 to 0.15 eV.

Including only caged and quasidiffusive motion, our model adequately fits the experimental MSD, Fig. 1(b), with three free parameters:  $b$ ,  $D$ , and  $\omega_E$ . Typical values for the fit parameters were  $b = 1.3$ ,  $D = 4.0 cm^2$ , and  $\omega_E = 40.0 s^{-1}$ . If the long-time particle motion were pure diffusion, one would expect  $b = 1$ . Our result,  $b > 1$ ,

indicates a superdiffusive process which might be attributable to shear motion of particles near crystallite boundaries during rotational domain slipping [4].

In order to extract further information from  $\omega_E$ , we assume that the interparticle potential is of Yukawa type:  $\phi_i = Q/r \exp(-\kappa)$ . The parameters entering the potential are the particle charge  $Q$ , distance from the particle  $r$ , and the screening strength  $\kappa = a/\lambda$ , where  $\lambda$  is the Debye screening length. For the Yukawa potential, assuming an ideal triangular lattice and summing Eq. (3) over nearest neighbors only, we have

$$\omega_E^2 = \frac{3Q^2}{ma^3} \exp(-\kappa) (1 + \kappa + \kappa^2). \quad (5)$$

Equation (5) is valid for  $\kappa > 4$ ; for smaller values of  $\kappa$ , more particles need to be included in the summation of Eq. (3). This is easily done, and for the results presented here the summation was carried out over 20 sets of nearest neighbors yielding an error in  $\omega_E^2$  of less than 5% at  $\kappa = 1$ . A partial derivation of this result is given in Ref. [18].

We obtain an important element of the interaction potential, the charge  $Q$ , by inverting Eq. (5) and using the fit  $\omega_E$  values. Note that we must also assume a value for the screening strength  $\kappa$ , for which we do not have a direct measurement in this experiment. In Fig. 2, we illustrate the  $\kappa$  dependence of Eq. (5) by plotting  $Q/e$  versus  $\kappa$  for  $\omega_E = 40 s^{-1}$  (where  $e$  is the electron charge). Here, note also the difference in the curves at small  $\kappa$  depending on the number of particles included in the summation in Eq. (3).

In Fig. 3, we take  $\kappa = 1$  and  $\kappa = 2$  as representative values, consistent with previous experiments [19,20], as well as  $\kappa = 4$ , and present the computed charge numbers  $Q/e$  as a function of the damping rate  $\nu$ . We find that  $Q$  varies little with  $\nu$ , consistent with previous results [2]. The mean and standard deviation for all  $\nu$  is

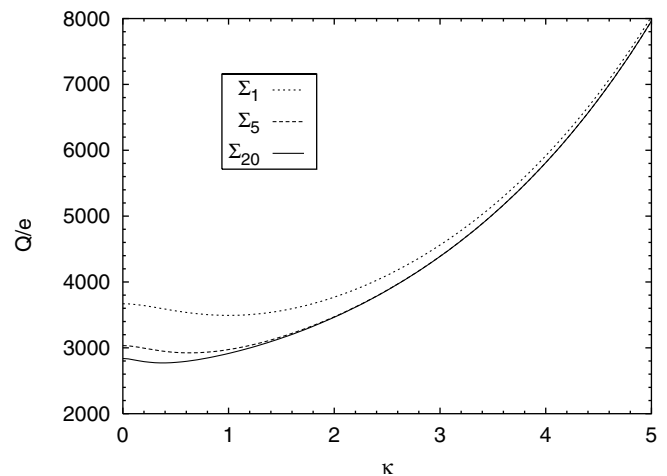


FIG. 2. Particle charge  $Q/e$  versus screening strength  $\kappa$  for  $\omega_E = 40 s^{-1}$  assuming a Yukawa interaction potential in a 2D lattice. Three curves are shown representing summations of Eq. (3) over 1, 5, and 20 sets of nearest-neighbor particles.

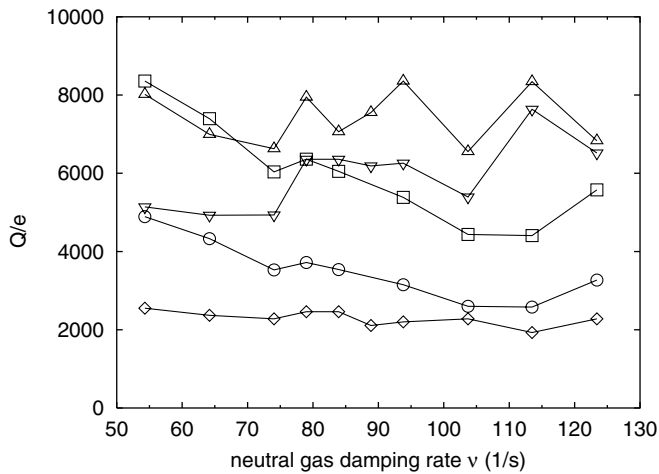


FIG. 3. Particle charge  $Q$  computed in three different ways: from the fit value of  $\omega_E$ , obtained from caged motion in the MSD, with  $\kappa = 2$  ( $\circ$ ) and  $\kappa = 4$  ( $\square$ ); from separate vertical resonance measurements ( $\triangle, \nabla$ ); and from an OML charging model using measured  $T_e$  (assuming  $n_e = n_i$ ,  $Q_{\text{OML}}/10$  plotted,  $\diamond$ ). The charge and screening length  $\kappa$  determine the interparticle potential in the Yukawa approximation.

$Q/e = 3000 \pm 200$  for  $\kappa = 1$ ,  $Q/e = 3500 \pm 300$  for  $\kappa = 2$ , and  $Q/e = 6000 \pm 400$  for  $\kappa = 4$ .

For comparison, two additional charge measurement techniques were carried out for the same experimental conditions. These results are also presented in Fig. 3. First, we measured the charge using the vertical resonance technique, where the resonance frequency of the vertical particle trap is measured and used to obtain the charge [21,22]. Second, we computed the charge from the orbit-motion limited (OML) model for particles in a flowing plasma. The results of this model for various plasma conditions are tabulated in Ref. [7]. Measured electron temperatures ( $T_e \sim 3$  eV) [8] and estimated ion temperature ( $T_e/T_i = 80$ ) and flow velocity (equal to the ion sound speed) were used to obtain this result for  $6.5 \mu\text{m}$  particles. Charge values obtained using these techniques are within an order of magnitude of those obtained using the caged motion technique. Note that none of these techniques are more accurate than a factor of 2 in measuring the charge due to various approximations. Other common charge measurement techniques, such as Mach cones [23] or horizontal compressional waves [18], are not practical here since they are primarily limited to low neutral pressure regimes ( $\leq 10$  mTorr) and monolayer crystals.

In summary, we have demonstrated a technique for characterizing the particle interaction potential directly from the observed particle dynamics. The caged-particle MSD yields the Einstein frequency of the lattice, which in turn yields information about the interparticle forces and po-

tentials. If one further assumes a particular form of the interparticle potential (e.g., Yukawa), parameters for that potential such as particle charge can then be extracted from the Einstein frequency. Since caged-particle motions occur naturally, this technique has the advantage that no external perturbation of the system is required in order to make the measurement.

We thank D. Samsonov, S. Nunomura, I. V. Schweigert, V. A. Schweigert, and A. Ivlev for helpful discussions. This work was supported by NASA, the National Science Foundation, and the Department of Energy.

\*Present address: Max-Planck-Institut für Extraterrestrische Physik, D-85748 Garching, Germany.

Electronic address:

†Electronic address:

- [1] H. M. Thomas and G. E. Morfill, *Nature (London)* **379**, 806 (1996).
- [2] A. Melzer, A. Homann, and A. Piel, *Phys. Rev. E* **53**, 2757 (1996).
- [3] C. A. Murray and R. A. Wenk, *Phys. Rev. Lett.* **62**, 1643 (1989).
- [4] W.-T. Juan and L. I., *Phys. Rev. Lett.* **80**, 3073 (1998).
- [5] T. G. Mason and D. A. Weitz, *Phys. Rev. Lett.* **74**, 1250 (1995).
- [6] H. Ohta and S. Hamaguchi, *Phys. Plasmas* **7**, 4506 (2000).
- [7] R. A. Quinn and J. Goree, *Phys. Rev. E* **61**, 3033 (2000).
- [8] R. A. Quinn and J. Goree, *Phys. Plasmas* **7**, 3904 (2000).
- [9] P. S. Epstein, *Phys. Rev.* **23**, 710 (1924).
- [10] M. J. Baines, I. P. Williams, and A. S. Asebiomo, *Mon. Not. R. Astron. Soc.* **130**, 63 (1965).
- [11] A. Melzer *et al.*, *Phys. Rev. E* **54**, R46 (1996).
- [12] V. A. Schweigert *et al.*, *Phys. Rev. Lett.* **80**, 5345 (1998).
- [13] U. Konopka, G. E. Morfill, and L. Ratke, *Phys. Rev. Lett.* **84**, 891 (2000).
- [14] F. Melandsø and J. Goree, *J. Vac. Sci. Technol. A* **14**, 511 (1996).
- [15] A. Melzer, V. A. Schweigert, and A. Piel, *Phys. Rev. Lett.* **83**, 3194 (1999).
- [16] V. A. Schweigert, I. V. Schweigert, V. Nosenko, and J. Goree (unpublished).
- [17] R. A. Quinn and J. Goree, *Phys. Rev. E* **64**, 051404 (2001).
- [18] A. Homann *et al.*, *Phys. Lett. A* **242**, 173 (1998).
- [19] U. Konopka, L. Ratke, and H. M. Thomas, *Phys. Rev. Lett.* **79**, 1269 (1997).
- [20] A. Homann, A. Melzer, and A. Piel, *Phys. Rev. E* **59**, R3835 (1999).
- [21] A. Melzer, T. Trottenberg, and A. Piel, *Phys. Lett. A* **191**, 301 (1994).
- [22] T. Trottenberg, A. Melzer, and A. Piel, *Plasma Sources Sci. Technol.* **4**, 450 (1995).
- [23] D. Samsonov *et al.*, *Phys. Rev. Lett.* **83**, 3649 (1999).